

# SEISMIC BEHAVIORS OF EARTH-CORE, CONCRETE-FACED-ROCK-FILL, AND COMPOSITE DAMS

D.S. Kim

*Korea Institute of Science and Technology (KAIST), Professor*

M.K. Kim

*HYUNDAI ENGINEERING Co., LTD.*

S.H. Kim

*Korea Institute of Science and Technology (KAIST), Master Candidate*

Y.W. Choo

*Korea Institute of Science and Technology (KAIST), Research Professor*

**Abstract:** The investigation on the seismic behavior of dams becomes crucial but is limited due to lack of experimental or field data. This paper aims to experimentally simulate the seismic behavior of three types of dams; earth-core rock-fill dam (ECRD), concrete-faced rock-fill dam (CFRD), and composite dam which combines concrete dam and CFRD. A series of staged centrifuge tests was performed by applying real earthquake record from 0.05g to 0.5g. The distributions of amplification ratio differed depending on the magnitude of earthquake loading, zoning condition, and dam type. The residual settlements and horizontal displacement at the dam crest were small but shallow surface sliding was dominant. The behavior of composite dam is also compared with the behaviors of CFRD.

**Keywords:** Dynamic centrifuge test, Earth-core rock-fill dam, Concrete faced rock-fill dam, Composite dam, Seismic behavior, Earthquake

## 1 INTRODUCTION

Over the past few decades, large number of ECRDs (earth-core rock-fill dams) and CFRDs (concrete-faced rock-fill dams) have been constructed and utilized over the world. These dams have been exposed in danger with recent strong earthquakes in many seismic regions, including Chile, Japan and China. In this region, damage to these dams has also been reported but most of them are manageable (Krinitzsky et al., 2002; Zhang et. al., 2010). However, the potential risk of seismic consequence still has aroused public deep concerns because the failure of dam can become critical threat to public safety.

One of the most important factors for the seismic safety of the dam is a dynamic response. The different composition of the dams affects the seismic response of the dams including the amplification characteristics, deformation of the dam, and stress on the concrete face slab. There are many types of the dams consisting of different composition or zones; the ECRD consists of permeable rock-fill zones and a very low permeable clayey core zone, and the main body of the CFRD consists of mostly rock material and reinforced concrete face slab on upstream slope for waterproofing. A composite dam, which is being constructed in Korea due to special geological conditions of a dam foundation, is another dam type with different composition because the composite dam combines a concrete dam and a CFRD. Especially in the composite dam, the seismic behavior of the joint of two different types of the dams will be quite complicated. In spite of the complex seismic response due to different composition, evaluations of seismic behavior of dam have relied mostly on theoretical and numerical analyses (Gazetas, 1987; Uddin, 1999). Furthermore, the seismic behavior of those dams still has remains not well understood.

This paper aims to experimentally simulate dams and evaluate the seismic behavior of dams by performing dynamic centrifuge tests. Three centrifuge model tests were performed to simulate the ECRD,

the CFRD, and the composite dam. The material properties of the core and the rock-fill were controlled to represent the average material properties of existing dams in Korea. Accelerometers were embedded in the model embankment as arrays to investigate the amplification of the ground motion. Laser sensors and a high speed camera were also mounted to measure the vertical settlement and horizontal displacement, respectively. Strain gages were attached on both sides of the CFRD facing to evaluate the axial force and moment during the earthquake. A series of staged tests was performed on the dam models with real earthquake record whose acceleration magnitude ranged from 0.05g to 0.5g. Based on the test results, the amplification characteristics, horizontal and vertical deformation of the dam body, stress distribution induced in the facing of the CFRD, and joint behavior of the composite dam were analyzed.

## 2 CENTRIFUGE TESTING PROGRAM

### 2.1 KAIST Centrifuge and Earthquake Simulator

The maximum capacity of KAIST beam centrifuge, with a 5m radius, is 2400kg for up to 100g of centrifugal acceleration. Earthquake loading can be simulated by an in-flight earthquake simulator equipped with an electro-hydraulic system. The earthquake simulator can simulate maximum ground acceleration of 0.5g into a prototype at a centrifugal acceleration of 40g (Kim et al., 2006).

### 2.2 Model Preparation

In this study, three types of Korean dams: ECRD, CFRD and a composite dam were investigated. Based on a database of existing dams in Korea, typical cross-sections of the three models were designed. Figure 1.a and Figure 1.b show the designs of the ECRD and the CFRD models, respectively. The slope of the ECRD model was 1:1.7 and the slope of the CFRD model was 1:1.4. A composite dam was modeled as shown in Figure 2. A concrete part of the composite dam had a slope of 1:0.7, and a rockfill model had a 1:2.0.

The model setups and the instrumentation of both the ECRD and CFRD are depicted in Figure 1. A scaling ratio (N) of 40 (referring to the centrifuge acceleration) was selected. The ECRD model is 130 mm high, simulating 5.2m high in a prototype scale. The CFRD model is 160 mm high, simulating 6.4 m high in a prototype scale. The model setup and the instruments of the composite dam is shown in Figure 2. The composite dam model is 148mm high for a 5.84m prototype dam with the scaling ratio of 40. The sizes of the models are relatively small compared to those of actual dams due to the limitations of the container size and the centrifugal acceleration capacity. Therefore, this study aims to provide experimental scheme and qualitatively evaluate seismic behaviors of the dams during earthquakes.

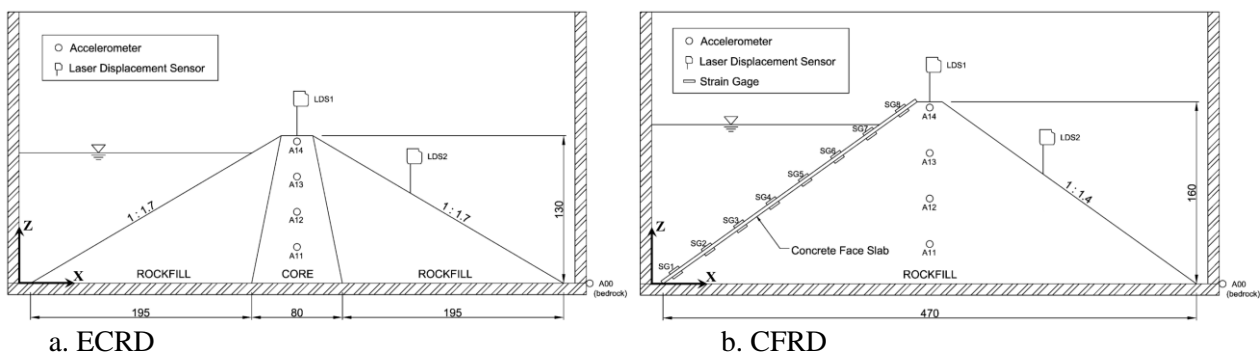
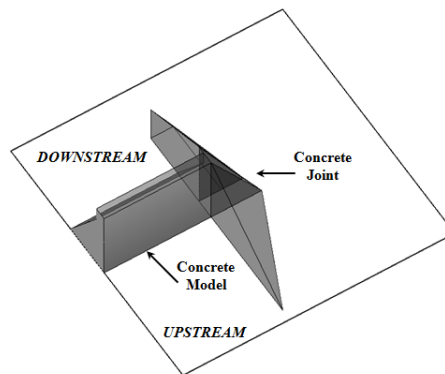
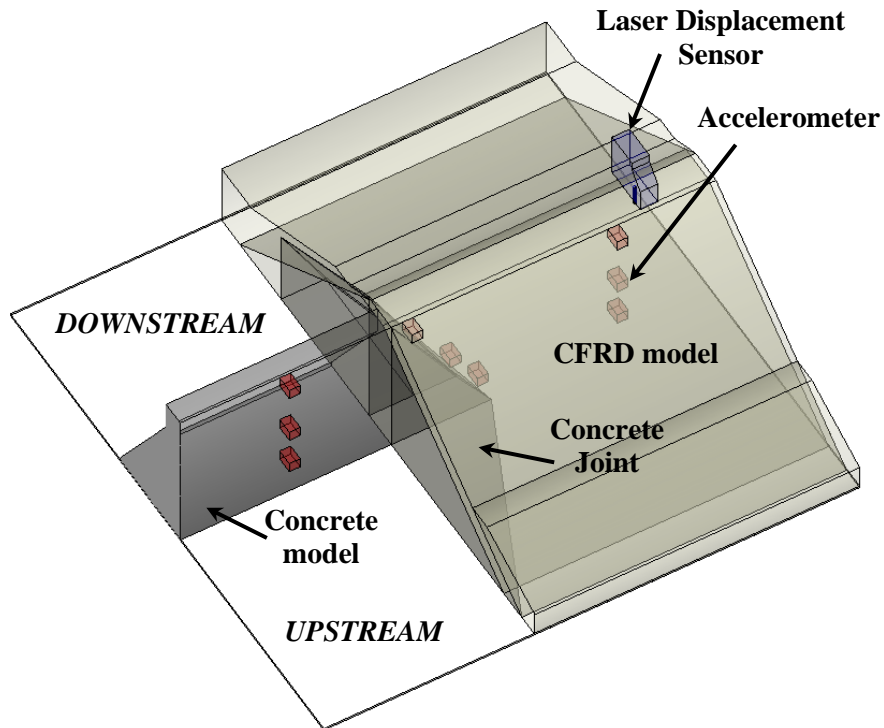
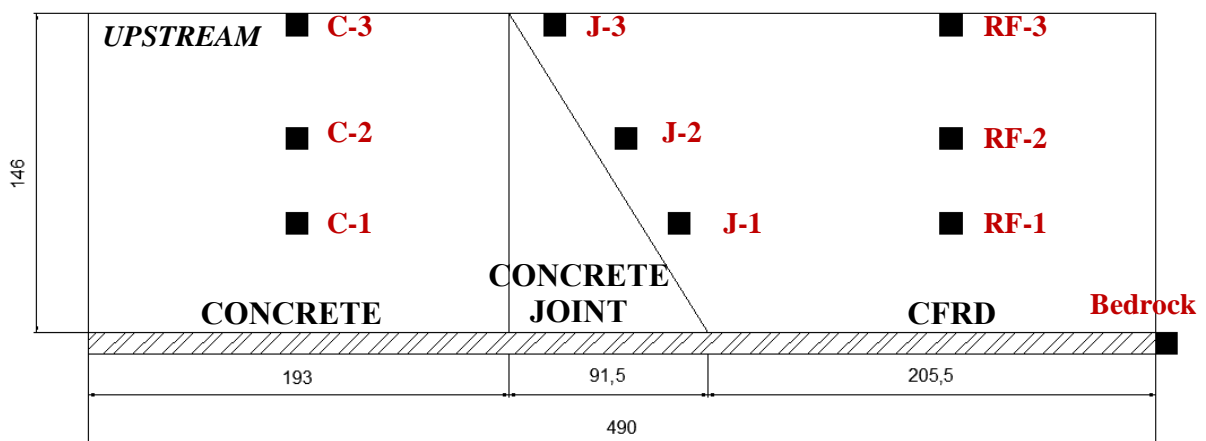


Figure 1. Layouts of model dams and instrumentation in the model scale



a. A bird-view

b. A bird-view of the concrete model



c. A view from the upstream side with accelerometers

Figure 2. Layouts of the composite model dam and instrumentation in the model scale

The CFRD model considers only the rock-fill zone whereas the ECRD model consists of rock-fill and core zones, the composite dam model had a concrete and rock-fill part. The rock-fill zones for three

types of dams were constructed with rock-fill material collected from a dam construction site. Because the particle size of actual rock-fill material is too large, it had to be reduced to be suitable for small-scale model. The model rock-fill materials were constituted by sieving the in-situ rock-fill materials by 20mm sieve. The material was reduced by a similar particle distribution method in which the particle size distribution curves of the model were parallel to that of the prototype material (Figure 3), mainly attempting to simulate its original properties properly, especially its mechanical deformation property (Xu et al, 2006). In the case of the ECRD core material, it was difficult to obtain a sample from a dam site. Hence, the core material was constituted by mixing clean sand and silica silt to meet the Korean standard specification for a core zone which should contain more than 20% of fine material finer than 0.1mm.

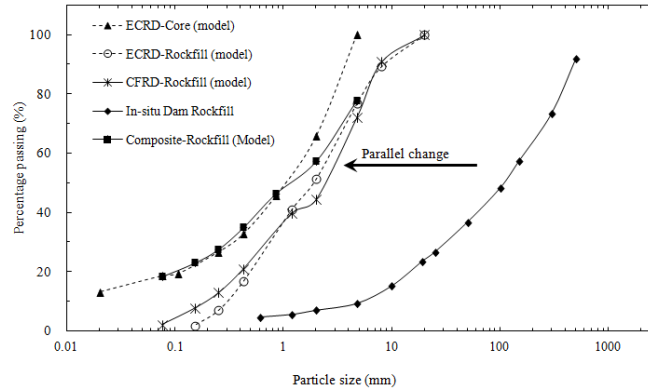


Figure 3. Particle size distribution curves of the prototype and model materials

The concrete part in the composite dam was made to simulate concrete gravity dam. The mold for the concrete model was made of pieces of steel plates so that both the concrete model and the concrete joint were monolithically casted. A concrete paste was mixed with the ratio of water: cement: concrete = 1: 2: 6. The steel mold was separated from the cured concrete model after three weeks and this model was attached to the baseplate of a model container by adhesive.

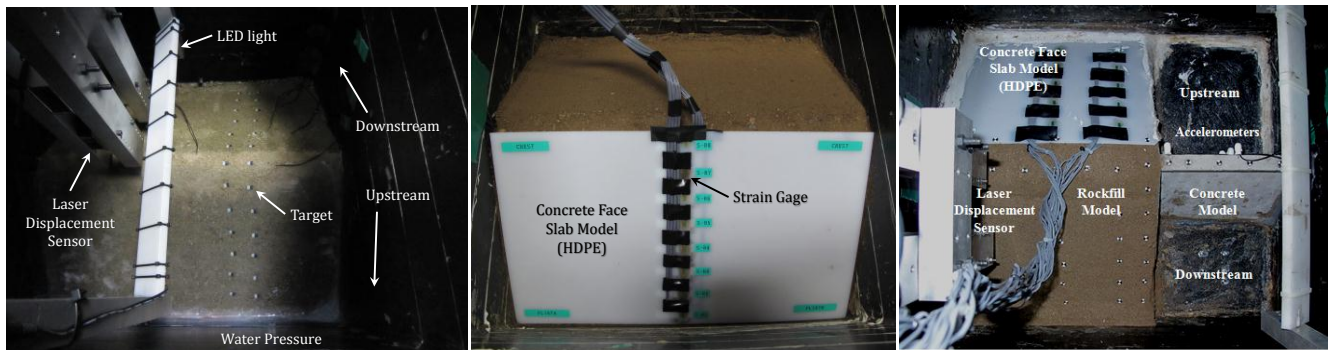
Because dams are mostly constructed on top of bedrock in Korea, the dam models were constructed directly on the baseplate of the model container. In order to simulate enough friction between the bedrock and the dam body, the model dams were constructed on the glued sandpaper. In case of the composite dam, only the area, where the rock-fill model was later placed, was covered by sandpaper. The side walls of the container were covered with grease to minimize side friction, resulting in a plane strain condition. The models were constructed with five layers to keep the densities uniform and compacted to 95% relative compaction by a hand compactor at an approximate compaction energy of 750kN·m/m<sup>3</sup>.

In the case of the CFRD and the composite dam, the face slab models were placed on upstream slopes to simulate the concrete face slabs. In the reduced model tests, it was difficult to use concrete material to model the bending stiffness of the face slabs in the prototypes. Therefore, the face slab models were made of high-density polyethylene (HDPE). Considering the scaling law, the thickness of the models was determined by the following equation (Zhang et al., 1994):

$$t_m = \sqrt[3]{\frac{E_p}{E_m} \frac{t_p}{N}} \quad (1)$$

Here,  $E_p$ ,  $E_m$ ,  $T_p$  and  $N$  are the elastic modulus of the prototype, the elastic modulus of the model, the thickness of the prototype slab and the scale ratio, respectively. The elastic modulus is 28GPa for the concrete face slabs and 1.2GPa for the HDPE. Based on the thickness of the prototype face, which is reduced at the same ratio of the dam size, the required thickness of the model was about 3mm.

A thin membrane was placed on the upstream slopes of the dam models, and the bottom and sides of the membrane were glued onto the rigid container to prevent water from penetrating into the dam body, allowing water to be contained in the upstream side. Therefore, the filled water imposed a water load on the upstream slope during the earthquake simulation. The seepage flow inside the dam body was not considered in this study because the study aims to investigate the seismic response of the typical dam types. The completed models are shown in Figure 4.



a. ECRD

b. CFRD

c. Composite dam

Figure 4. Photographs of the constructed models

### 2.3 Testing and Monitoring Program

Earthquake input motion was excited at the base of the rigid container containing each dam model. The Ofunato earthquake record was used as the upstream-downstream input motion in this study, as a short period dominant earthquake is most probable in regions of Korea. To monitor the seismic behaviors of the models, various transducers were used, as shown in Figures 1 and 2. Stage tests were carried out successively for each dam model. The smallest peak acceleration was applied at the beginning and this was followed by successively higher input acceleration magnitudes, ranging from 0.04g to 0.5g .

In order to monitor the deformation of the dam body in the ECRD and the CFRD models, the vertical and horizontal displacement of the dam surface were measured. For vertical displacement, laser displacement sensors were adopted and hung over the dam crest to measure the settlement at the dam crest. For horizontal displacement, a high-speed camera was installed at the frame of the centrifuge arm, where the camera could capture the top view and horizontal displacement of the dam surface.

Accelerometers were embedded inside the ECRD and CFRD model dams to investigate acceleration amplification of the model dams. These accelerometers were placed at different depths underneath the crest of the dam as shown in Figure 1. Likewise, accelerometers for the composite dam model were used to obtain acceleration amplification and those accelerometers were aligned with the crest at different depths. For the composite dam model, three arrays of the accelerometers were located at the positions shown in Figure 2; the first array was on the concrete model, the second was near the joint in the rock-fill model, and the last one was in the center of the rock-fill. The arrays were used to evaluate the comparative seismic responses at each location.

In the case of the CFRD, eight pairs of strain gages were attached onto both sides of the face slab to measure the bending moments and axial forces. Each strain gage was wired up in a quarter bridge circuit so that the outer and inner circumferential strains were obtained. Measured strain gage data were converted to the bending moment and axial force in a prototype scale.

### 3 TEST RESULTS AND DISCUSSIONS

#### 3.1 Seismic behavior of the ECRD and the CFRD

##### 3.1.1 Acceleration Measurements

The peak acceleration distributions with the dam height at four different earthquake levels and their normalized distributions are shown in Figure 5. In the case of the ECRD, the peak acceleration increased continuously from the bedrock to the dam crest at about 0.1g of bedrock acceleration. At higher bedrock acceleration, the amplification factors in the lower part of the dam does not change much, however, the amplification ratios in the upper part show large increase with the height. The amplification ratio distribution of the CFRD showed the similar increasing trend to the ECRD at small bedrock accelerations. The amplification ratio at the upper part shows a high increase at bedrock accelerations that exceed 0.4g, whereas the amplification ratio does not change much in the lower part.

When the maximum bedrock acceleration of 0.57g was excited, the amplification ratio between the base and the crest increased significantly to almost 3.4 in the CFRD. It is postulated that this considerable amount of amplification was caused by the loosening of the upper part of the embankment because the considerable settlement was recognized at this earthquake. Once some part of the dam body loosens, the particles move more freely because the resistance against the movement of the soil particles decreases. Therefore, the loosening effect of the embankment material can cause significant amplification of the ground acceleration. This loosening corresponds to the deformation results. This will be discussed again with the deformation results in the next part of the paper.

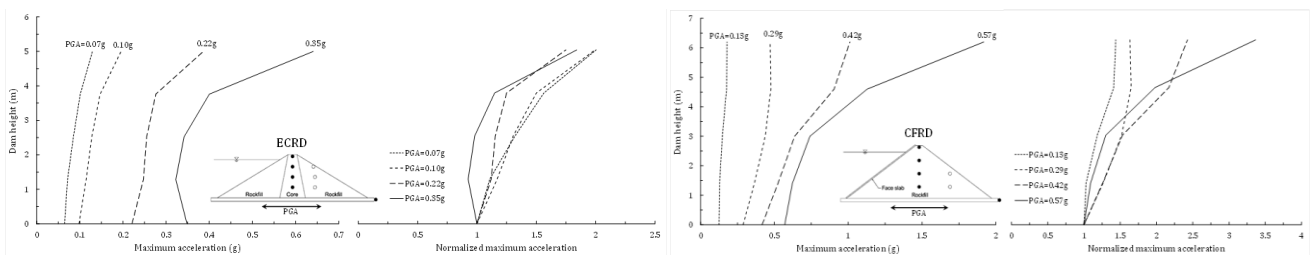


Figure 5. Maximum acceleration and normalized acceleration distribution at the center for the centrifuge tests (in the prototype scale)

##### 3.1.2 Settlement and Horizontal Deformation

During the stage tests, settlements of the model dams were continuously measured by laser displacement sensors, and residual settlement amounts were obtained after each test. The cumulative settlements of the crest residual settlements are shown in Figure 6. In the case of the ECRD model, the dam body began to settle from the input bedrock acceleration of 0.1g. Relatively small settlements were recorded in the event of small earthquakes (from 0.1g to 0.2g). Finally, a large amount of settlement was recorded after the maximum bedrock acceleration of 0.35g. The settlement of the ECRD corresponds to the amplification characteristics, showing higher amplification in the upper part of the dam at more than 0.2g acceleration (Figure 6). This settlement and the corresponding amplification at the upper part were more likely caused by the silty core material in the ECRD model when the silty material started to yield.

On the other hand, there were very small settlements at the crest in the CFRD model until 0.37g of input bedrock acceleration. Subsequently, large negative settlement (heaving) occurred in a range from 0.37 to 0.45g, followed by considerable positive settlement at the last shaking. This heave was likely caused by the loosening of the rock-fill material that was densely constructed. During the preparation of the model, the rock-fill zone was compacted to a very dense state. As earthquake loadings were excited, the densely compacted soil particles started to move, resulting in a change of the soil density in the rock-

fill zone. Once the densely compacted particles overcame the adjacent particles to move, the upper part of the dam dilated and became loose. After this loosening, the amplification of acceleration significantly increased at the upper part due to the loosening of the rock-fill material, resulting in the large settlement amount and the surface sliding toward the downstream direction, as was observed in Figure 7.

When the highest amount of settlement was noted, the recorded residual crest settlements were 9.72mm in the ECRD model (under a maximum bedrock acceleration of 0.348g) and 13.36mm in the CFRD (under a maximum bedrock acceleration of 0.570g). These settlements amount 0.19% of the dam height in the ECRD and 0.21% of the dam height in the CFRD. The ratio of the settlement to the dam height has been a useful parameter to quantify dam damage because the settlement reflects deformation of dam body, sliding, cracking and so on (Swaisgood, 2003).

The horizontal displacement histories at two points at the crest and slope were obtained by an image processing technique. In the case of the ECRD, the maximum horizontal displacements were 4.99mm (0.096% of the dam height) at the dam crest and 1.32mm (0.025% of the dam height) at the downstream slope. The maximum horizontal displacement was approximately half of the maximum crest settlement (9.72mm) in the same test. In the case of the CFRD, the maximum horizontal displacements were 51.2mm (0.80% of the dam height) at the dam crest and 14.1mm (0.22% of the dam height) at the downstream slope. These values imply that a small amount of sliding toward the downstream direction occurred. It is interesting to note that shallow sliding toward the downstream direction occurred especially on the surface during the shaking and this was the most severe damage in this study, even under 0.5g of maximum bedrock acceleration.

In addition, the photographs taken by the high speed camera clearly revealed these shallow surface sliding tendencies (Figure 7). In the downstream surface of the model, a large amount of soil and rock materials fell down toward the downstream direction. This sliding and the loosening phenomenon observed above are very comparable to the field observation of the Zipingpu dam, which experienced the May 12, 2008 Wenchuan earthquake. In the report, the paved rock blocks on the downstream slope of the Zipingpu dam were uplifted and loosened, and a few of the blocks were scattered on the downstream slope (Zhang et al., 2010).

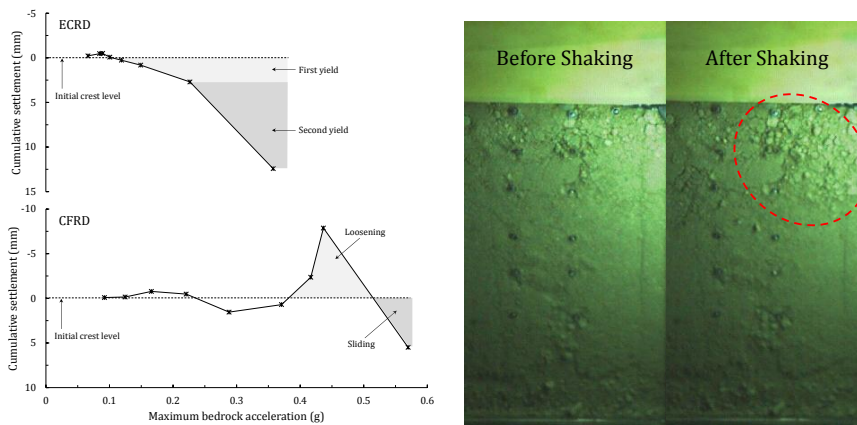


Figure 6. Cumulative settlement histories with increasing maximum bedrock accelerations (left)

Figure 7. Photographs of the downstream slope of the CFRD model after 0.57g bedrock motion was excited (right)

### 3.1.3 Induced Stresses on CFRD Facing

The strains of the face slab were measured during the increase of the centrifugal acceleration (static condition) and the application of earthquake loading (dynamic condition). Figure 8 shows the tensile stress increment by earthquake. These the results show that the tensile stress increments on both the outer and inner faces increased slightly to the maximum base acceleration of about 0.4g. The tensile stress

increment then rapidly increased especially at SG7 (h=5.28m). This rapid change in the face slab response corresponds to the embankment loosening behavior discussed in the previous section.

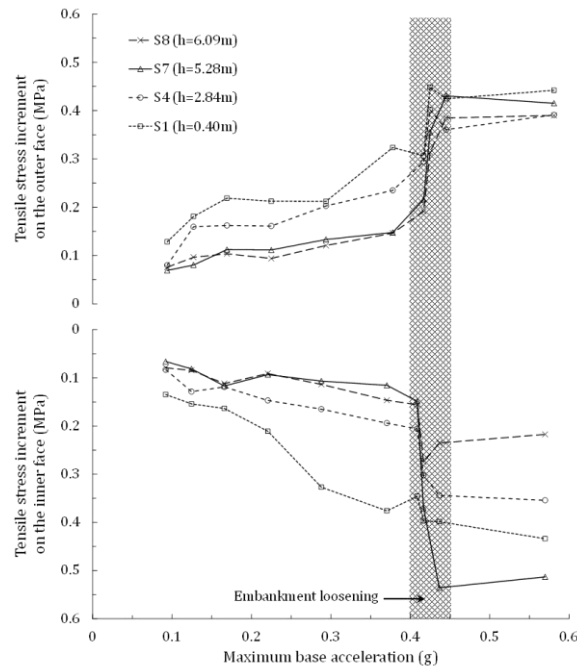
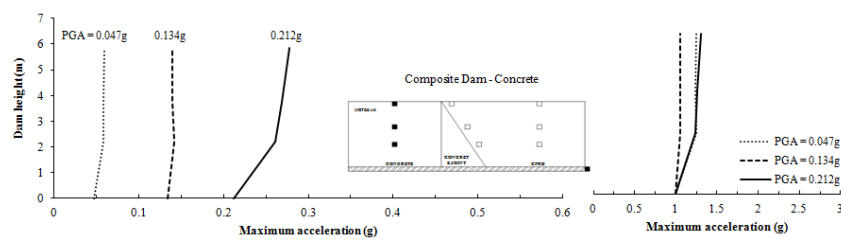


Figure 8. Tensile stress increments on the outer and inner surfaces of the face slab

### 3.2 Seismic Behavior of the Composite Dam

Figure 9 shows the variations in peak acceleration with depth measured at the concrete model, the joint, and the center of the rock-fill model. When the bedrock PGA was 0.212g, the data of the crest acceleration at the rock-fill model was missed due to problems in data acquisition process. In the center of the rock-fill model, the peak acceleration increased from the bedrock to the crest, and the amplification at the crest increased significantly as the bedrock accelerations increased. In general, the amplification pattern of the rock-fill model away from the concrete joint of the composite dam model was similar with the amplification pattern of the CFRD dam model.

It is interesting to note that the peak accelerations at the joint were different from those at the center of the rock-fill model. The amplification ratio distribution trend of the joint was also different from the trend of the center of the rock-fill model. In the center of the rock-fill model, the amplification ratios at the crest showed high whereas the amplification ratios at the lower part did not change significantly. Considering that the concrete model was not amplified much with the depths, the joint shows the amplification trend between the CFRD model and the concrete model.





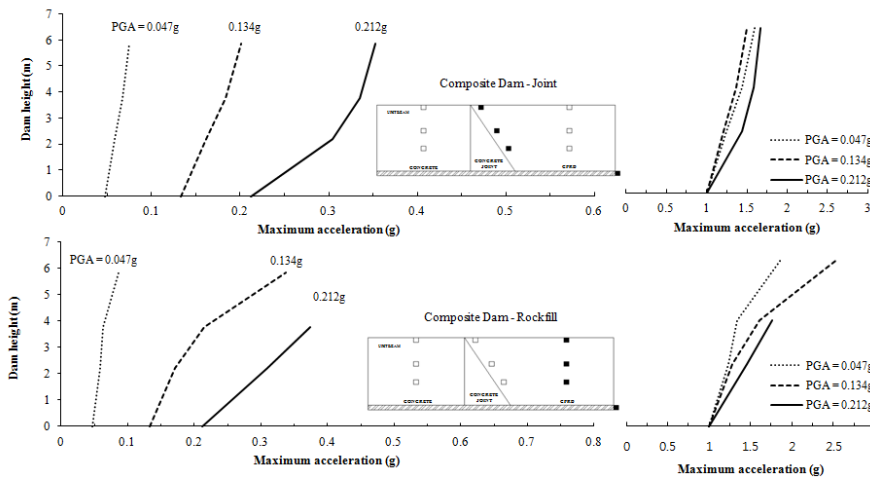


Figure 9. Maximum acceleration and normalized acceleration distribution at the concrete model, the joint, and at the center of the rock-fill model of the composite dam (in the prototype scale)

Figure 10 shows the acceleration-time histories between 4.4 sec to 4.8 sec at different depths of the concrete model, the joint, and the rock-fill model. The signals from the accelerometers in the concrete model coincided. However, the acceleration records at different depths of the rock-fill model were asynchronous and the magnitudes of the acceleration increased as the heights of the accelerometers increased. The acceleration of the joint was less asynchronous than the acceleration of the rock-fill dam was. Also, the magnitudes of the acceleration in the joint were lower than those of the rock-fill dam as discussed in Figure 9.

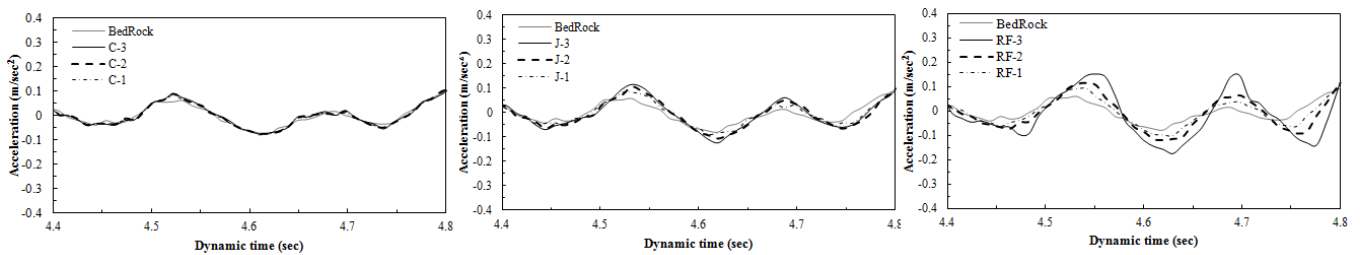


Figure 10. Acceleration records at different heights of the concrete model (c), the joint (J), and the rock-fill model (RF) (in the prototype scale)

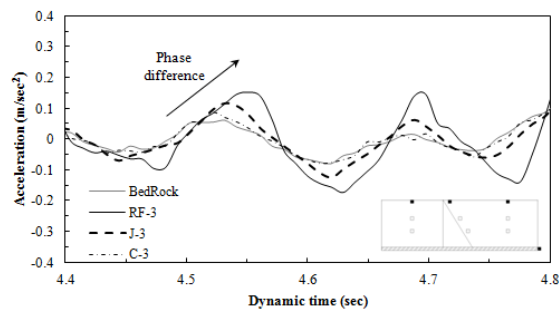


Figure 11. Acceleration records at the crest of concrete model, the joint, and the rock-fill model (in the prototype scale)

In order to compare the behaviors among concrete model, joint, and rock-fill model effectively, records of the acceleration-time histories at the crest are shown in Figure 11. It is interesting to note that there exists a phase difference among the bedrock, the concrete model, the joint, and the rock-fill model. The magnitudes of the accelerations and the phase differences were increased in sequence as the bedrock, the concrete model, the joint and the rock-fill model. Especially the acceleration of the concrete model was almost synchronous with the acceleration of the bedrock. The acceleration record of the rock-fill

model had the highest amplitude of the acceleration and the biggest phase difference. The phase difference and the magnitude of the acceleration of the joint were intermediate between the joint and the rock-fill model. Therefore, it can be noticed that the joint can be considered to have a characteristics in the seismic behavior between the concrete dam model and the rock-fill model.

Based on the physical modeling, the seismic response of the joint in a composite dam can be effectively investigated and further data reduction on relative displacement between concrete model and rock-fill model is under development. It shows the advantages of physical modeling in the estimation of complex interaction behavior because it would be quite difficult to simulate the similar behavior numerically.

## 4 CONCLUSIONS

In this study, three centrifuge model tests were performed to simulate the seismic behaviors of a earth-cored rock-fill dam (ECRD), a concrete-faced rock-fill dam (CFRD), and a composite dam which combines the concrete dam and CFRD. The detailed modeling and monitoring techniques of three different type dams were discussed. A series of staged centrifuge tests was performed by applying real earthquake record from 0.05g to 0.5g. The distributions of amplification ratio differed depending on the magnitude of earthquake loading, zoning condition, and dam type. The residual settlements and horizontal displacement at the dam crest were small but shallow surface sliding was dominant. The behaviors of the joint area in the composite dam were investigated in terms of amplification and phase characteristics showing the intermediate behaviors between concrete dam and CFRD models.

## ACKNOWLEDGEMENT

This research was supported by the Basic Science Research Program through the National Research Foundation of Korea (NRF) funded by the Ministry of Education, Science and Technology (Grant number: 2009-0080575).

## REFERENCES

- E.L. Krinitzsky, M.E. Hynes, The Bhuj, (2002). India, earthquake: lessons learned for earthquake safety of dams on alluvium, *Engineering Geology* 66 163-196.
- J.M. Zhang, Z.Y. Yang, X.Z. Gao, Z.X. Tong, (2010). Lessons from damages to high embankment dams in the May 12, 2008 Wenchuan earthquake, *Proceedings of the 2010 GeoShanghai International Conference*.
- D.S. Kim, G.C. Cho, N.R. Kim, (2006). Development of KOCED geotechnical centrifuge facility at KAIST, *Proceedings of International Conference on Physical Modelling in Geotechnics*, pp.147-150.
- G. Gazetas, (1987). Seismic response of earth dams: some recent developments, *Soil Dynamics and Earthquake Engineering*, 6 (1) 2-47.
- N. Uddin, (1999). A dynamic analysis procedure for concrete-faced rockfill dams subjected to strong seismic excitation, *Computers and Structures*, 72 409-421.
- L. Zhang, T. Hu, J. Zhang, (1994). Evaluation of the cut-off structures of a rockfill dam, *Proceedings of the International Conference Centrifuge 94*, pp. 593-598.
- Z. Xu, Y. Hou, J. Liang, L. Han, (2006) Centrifuge modeling of concrete faced rockfill dam built on deep alluvium, *Proceedings of International Conference on Physical Modelling in Geotechnics*, pp. 436-440.
- J.R. Swaisgood, (2003). Embankment dam deformations caused by earthquakes, *Proceedings of the 2003 Pacific Conference on Earthquake Engineering*, Christchurch NZ.
- Mu-Kwang Kim, Sei-Hyun Lee, Yun Wook Choo, Dong-Soo Kim, (2011). Seismic behaviors of earth-core and concrete-faced rock-fill dams by dynamic centrifuge tests, *Soil Dynamics and Earthquake Engineering*, 31 1579-1593.